Supplementary Information

Ion induced ferromagnetism combined with self-assembly for large area magnetic modulation of thin films

Michal Krupinski*[a], Rantej Bali[b], Dmitriy Mitin[c], Pawel Sobieszczyk[a], Jakub Gregor-Pawlowski[a,d], Arkadiusz Zarzycki[a], Roman Böttger[b], Manfred Albrecht[c], Kay Potzger[b], Marta Marszałek[a]

[a]Institute of Nuclear Physics Polish Academy of Sciences, Radzikowskiego 152, 31–342 Kraków, Poland

[b]Helmholtz-Zentrum Dresden-Rossendorf, Bautzner Landstrasse 400, 01328 Dresden, Germany

[c]Institute of Physics, University of Augsburg, Universitätsstraße 1, 86135 Augsburg, Germany

[d]AGH University of Science and Technology, Faculty of Physics and Applied Computer Science, al. Mickiewicza 30, PL-30059 Kraków, Poland

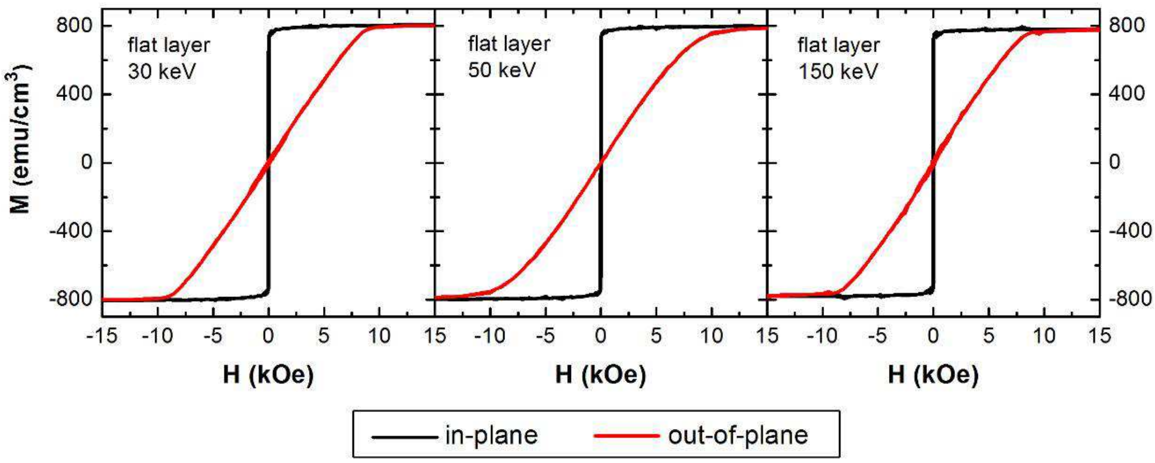

Figure S1. Hysteresis loops measured by SQUID magnetometry at room temperature for flat reference samples irradiated by Ne^{+} ions with energy of (a) 30 keV, (b) 50 keV, and (c) 150 keV. The shape of the loops is very similar irrespective from the used energy. All the samples show strong magnetic anisotropy, caused by shape anisotropy, with magnetization easy axis lying in the sample plane. Anisotropy field H_a for all reference samples amounts of about 9 kOe, while coercivity field H_C is about 50 Oe for the in-plane measurement geometry and nearly zero for the out-of-plane configuration.

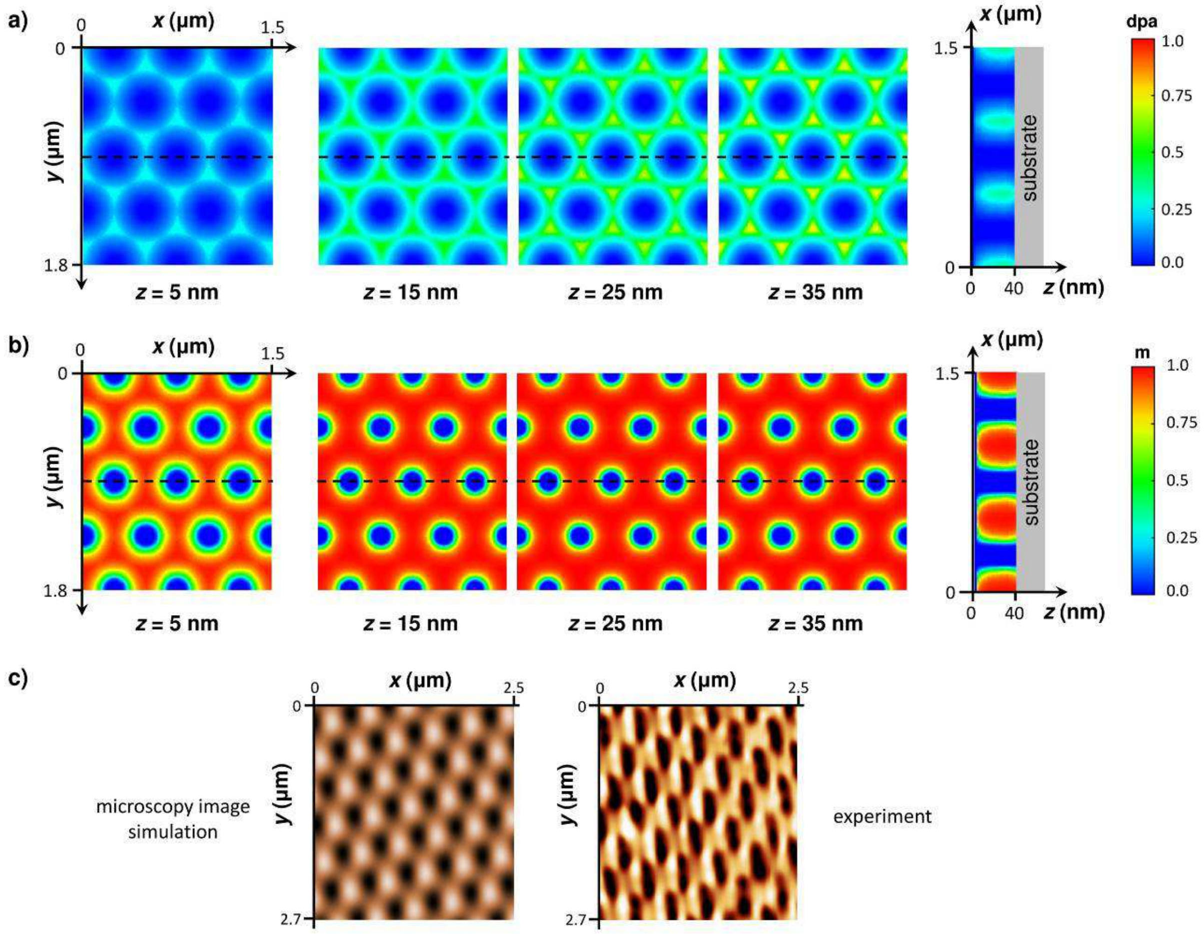

Figure S2. (a) Simulated distribution of changes in the $Fe_{60}Al_{40}$ alloy structure (displacements per atom - dpa) for the film irradiated through a polystyrene mask with a period of 508 nm; four exemplary distributions for different depth (*z*) are shown; the figure on the right shows the depth cross-section along the dotted line marked in the images; (b) distribution of induced magnetic moment (normalized) calculated on the basis of the corresponding dpa distribution maps; the figure on the right shows the depth cross-section of the map along the dotted line marked in the images; (c) simulated map of the perpendicular component of the stray field 200 nm above the sample surface in the saturated state and comparison with the corresponding SMRM image.

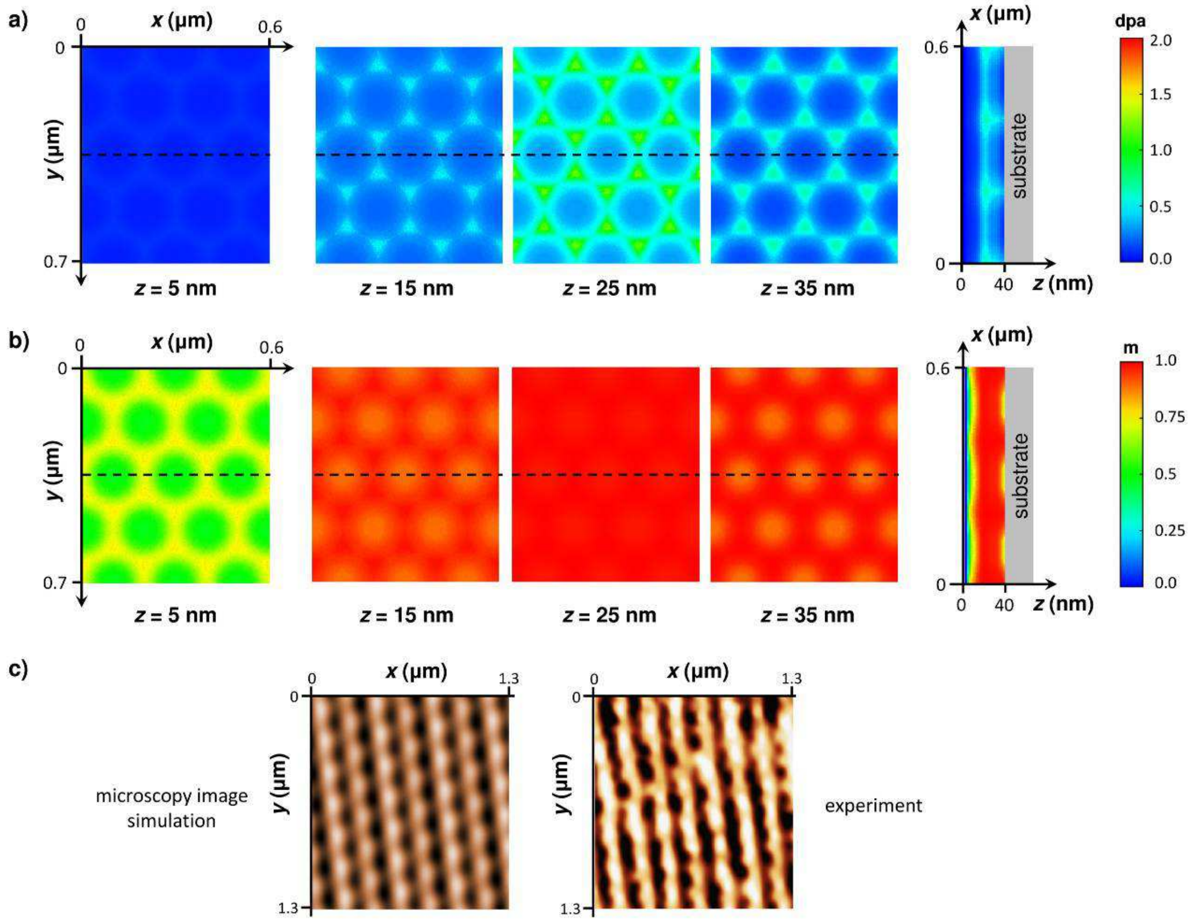

Figure S3. (a) simulated distribution of changes in the $Fe_{60}Al_{40}$ alloy structure (displacements per atom - dpa) for the film irradiated through a polystyrene mask with a period of 202 nm; four exemplary distributions for different depth (*z*) are shown; the figure on the right shows the depth cross-section along the dotted line marked in the images; (b) distribution of induced magnetic moment (normalized) calculated on the basis of the corresponding dpa distribution maps; the figure on the right shows the depth cross-section of the map along the dotted line marked in the drawings; (c) simulated map of the perpendicular component of the stray field 200 nm above the sample surface in the saturated state and comparison with the corresponding SMRM image.

X-Ray Reflectivity (XRR) measurements

The structure of the samples was studied by X-Ray Reflectivity measurements carried out with X'Pert Pro Panalytical diffractometer equipped with vertical goniometer and copper x-ray tube (2.2 kW, Cu $K_{\alpha 1}$ with λ = 1.54056 Å). The incident beam optics was composed of Soller (0.04 rad) and 1/32 deg divergence slits with lateral width limited by 5 mm mask. The 0.125 mm thick Ni filter was also included to cut-off a Cu K_{β} (λ = 1.39225 Å) line. Reflected beam path was formed by Soller (0.04 rad), parallel plate collimator with equatorial acceptance of 0.18 deg, and collimator slits (0.27 deg), and the data were collected by proportional counter. Figure S4 shows the x-ray reflectometry pattern for annealed $Fe_{60}Al_{40}$ layer.

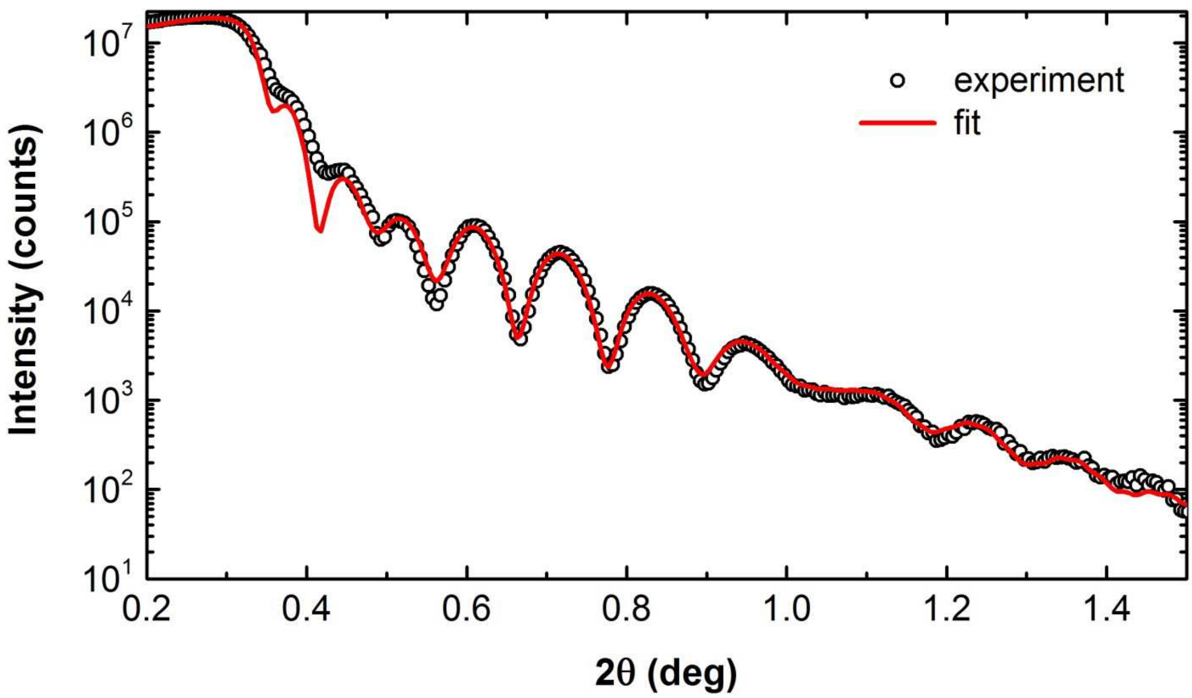

Figure S4. X-ray reflectivity curve for annealed $Fe_{60}Al_{40}$ film. Points represent experimental data, while the line shows fit obtained using Parrat algorithm.

X'Pert Reflectivity program provided by PANalytical was used to fit and analyze measured reflectivity curve. Computer code of this software was based on Parratt recursion and the least squares fitting with segmented fitting algorithm. The fitted parameters were the substrate and layers roughness, and the thickness of $Fe_{60}Al_{40}$ layer and outer oxide film. The parameters obtained from this procedure are collected in Table T1.

layer	**density (g/cm^3)**	**thickness (nm)**	**roughness (nm)**
Si	2,33*	---	0,9 ± 0,5
SiO_2	2,64*	150*	1,0 ± 0,5
FeAl	5,64 ± 0,27	35,6 ± 0,7	1,6 ± 0,6
Fe-Al-O	3,82 ± 0,87	4,5 ± 0,8	1,5 ± 0,6

Table T1. Results of fitting reflectivity curve shown in Figure S4 for flat annealed $Fe_{60}Al_{40}$ layer. Values marked by * were fixed as constant during the whole fitting procedure.